

Linear optics compensation for the HEX superconducting wiggler at NSLS-II

Y. Li

To be published in "Journal of Physics: Conference Series"

February 2024

Photon Sciences

Brookhaven National Laboratory

U.S. Department of Energy

USDOE Office of Science (SC), Basic Energy Sciences (BES)

Notice: This manuscript has been authored by employees of Brookhaven Science Associates, LLC under Contract No. DE-SC0012704 with the U.S. Department of Energy. The publisher by accepting the manuscript for publication acknowledges that the United States Government retains a non-exclusive, paid-up, irrevocable, world-wide license to publish or reproduce the published form of this manuscript, or allow others to do so, for United States Government purposes.

DISCLAIMER

This report was prepared as an account of work sponsored by an agency of the United States Government. Neither the United States Government nor any agency thereof, nor any of their employees, nor any of their contractors, subcontractors, or their employees, makes any warranty, express or implied, or assumes any legal liability or responsibility for the accuracy, completeness, or any third party's use or the results of such use of any information, apparatus, product, or process disclosed, or represents that its use would not infringe privately owned rights. Reference herein to any specific commercial product, process, or service by trade name, trademark, manufacturer, or otherwise, does not necessarily constitute or imply its endorsement, recommendation, or favoring by the United States Government or any agency thereof or its contractors or subcontractors. The views and opinions of authors expressed herein do not necessarily state or reflect those of the United States Government or any agency thereof.

PAPER • OPEN ACCESS

Linear optics compensation for the HEX superconducting wiggler at NSLS-II

To cite this article: Yongjun Li *et al* 2024 *J. Phys.: Conf. Ser.* **2687** 062002

View the [article online](#) for updates and enhancements.

You may also like

- [The Latest Status of NSLS-II Insertion Devices](#)
Toshi Tanabe, Charles Kitegi, Ping He et al.
- [Lossless crossing of a resonance stopband during tune modulation by synchrotron oscillations](#)
G M Wang, T Shaftan, V Smaluk et al.
- [Fast glitch detection of coupled bunch instabilities and orbit motions](#)
Weixing Cheng, Belkacem Bacha, Kiman Ha et al.



ECS The Electrochemical Society
Advancing solid state & electrochemical science & technology

ECS UNITED

247th ECS Meeting
Montréal, Canada
May 18-22, 2025
Palais des Congrès de Montréal

Showcase your science!

Abstracts due December 6th

Linear optics compensation for the HEX superconducting wiggler at NSLS-II

Yongjun Li, Kiman Ha, Yoshiteru Hidaka, Robert Rainer, Timur Shaftan, Victor Smaluk, Toshiya Tanabe, Yuke Tian, Guimei Wang, Xi Yang

Brookhaven National Laboratory, Upton 11973, New York, USA

E-mail: yli@bnl.gov

Abstract. At the NSLS-II ring, a 1.2 m long superconducting wiggler with the maximum 4.34T magnetic field has been installed at a low- β straight section (cell 27) to drive the high energy engineering X-ray scattering (HEX) beamline. To mitigate the potential performance degradation due to the linear optics distortion, a local compensation scheme was adopted and confirmed with the online beam measurement. A feedforward control to enable a dynamic compensation of the linear optics distortion was deployed. It can maintain the storage ring lattice performance when the device main coil current ramps.

1. INTRODUCTION

A 1.2m long superconducting wiggler has been recently installed in the NSLS-II storage ring's 27th cell to drive the High Energy engineering X-ray scattering (HEX) beamline. However, the alternating magnetic field generated by the wiggler can cause a linear lattice distortion, particularly in the vertical plane, which might have a potentially negative impact on the performance of the ring lattice. The optics distortion can result in low injection efficiency and reduced beam lifetime because of a degradation of dynamic aperture (DA) and local momentum aperture (LMA). To address this issue, a local compensation scheme was designed and deployed to recover the linear optics distortion. Six neighboring quadrupoles were chosen to confine the optics distortion only within the straight occupied by the wiggler itself. When the wiggler field ramps to different peak values, these quadrupoles can dynamically compensate the optics distortion in the manner of a feedforward control. Besides the optics compensation discussed in this paper, an orbit compensation was also deployed to mitigate its first and second field integral errors and reported in the same proceedings [1].

2. Simulation and experimental studies

The linear optics in storage rings can be characterized by the Twiss functions $(\beta, \alpha)_{(x,y)}$ and the dispersion function $\eta_{(x,y)}$ respectively. Since this device is located in a non-dispersive straight section, and its intrinsic dispersion leakage of is negligible due to its periodical structure. Therefore, only the Twiss functions, particularly in the vertical plane, have large distortions. The concept of compensation is to confine the optics distortion within the straight, and make it transparent to the rest of the storage ring.



2.1. Simulation

The maximum peak field of this wiggler can reach up to 4.34T when its main coil is powered to 440 A for the routine operation, and the peak field variation with its excitation current is illustrated in Fig. 1. At $B_{peak} = 4.34T$, the device was modeled as a 2D transverse kickmap [2] and integrated into the storage ring lattice. Since it is off-centered downstream by 1 m in cell 27 straight (see Fig. 2, its up- and down-stream quadrupole compensations have to be asymmetric as well.

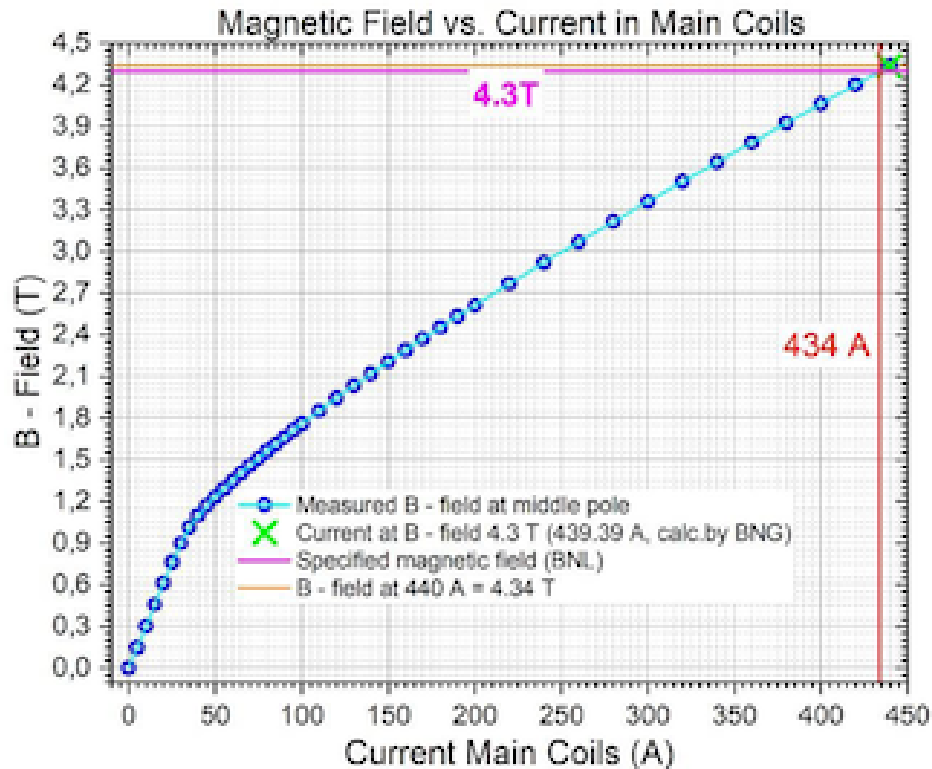


Figure 1. Vertical peak field B_y vs. main coil current of the HEX wiggler.

We solved the linear optics compensation scheme as the follow optimization problem. For a given beam-line segment from the exit of cell 26's last dipole to the entrance of cell 27's first dipole, with the initial Twiss functions $(\beta, \alpha)_{(x,y)}$ as the existing ring optics, we vary six independently powered quadrupoles as free knobs to let the Twiss functions at the exit to exactly match $(\beta, -\alpha)_{(x,y)}$. In the meantime, keeping the phase advances $\phi_{(x,y)}$ unchanged is used as constraint.

There are six constraints and six free knobs, and the solution should be unique. However, some soft constraints need to be considered as well, for example, the compensation ΔK_1 should be sufficiently weak so that new quadrupole settings are still within the capacity of their power supplies, and the maximum β -functions are limited within reasonable ranges. Since a global tune feedback is already in place in the NSLS-II ring, the constraints on the phase advance is loose. The optics after compensation is illustrated in Fig. 2, which confines the (β, α) distortion within the straight with some small quadrupole adjustments. The chromaticity change is so small that no change is needed for the chromatic sextupoles. The dynamic aperture and local momentum aperture were confirmed sufficient to satisfy the routine operation requirements (see Fig. 3) using the tracking code ELEGANT[3].

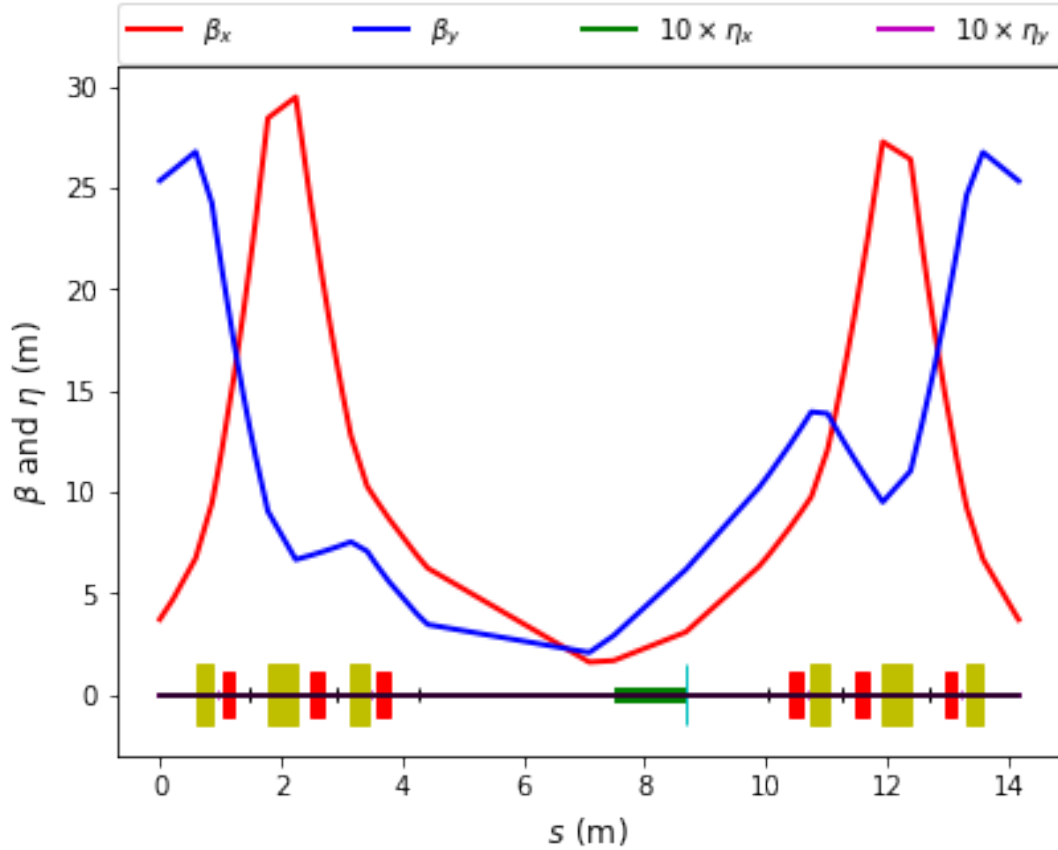


Figure 2. Magnet layout in cell 27 nondispersive straight and new β -functions after compensation. The green block is the wiggler; the yellow ones are quadrupoles, which are used as the compensation knobs, and the red ones are harmonic sextupoles. Since the maximum intrinsic dispersion inside the wiggler is only $70 \mu\text{m}$, it is not shown there.

2.2. Experimental studies

During the routine operation, this device can be turned on and off with a stored beam. In the worst scenario, the superconducting magnet quench might occur. Therefore, its main coil excitation current needs to ramp up and down occasionally. Consequently, its perturbation on the linear optics needs to be dynamically compensated with such changes. We experimentally calibrated the linear optics along the excitation curve as shown in Fig. 1 and generated a feedforward table in order to deploy dynamic compensation. Experimentally, it is impractical to directly measure the Twiss function exactly at the entrance and exit of cell 27 straight with beam. Alternatively, except 4 specific beam position monitors (BPM) located in cell 27 straight, other 176 β -functions were measured at the locations of BPMs along the ring. Then six quadrupoles neighboring to the device were used to minimize the optics distortions. In other words, rather than matching the Twiss (β, α) exactly at the entrance/exit of the straight, the β -beats observed by the rest ring (i.e., 176 BPMs) were chosen as the correction objective to make the wiggler transparent. Finally, based on the measurements, the needed compensation for six quadrupoles were computed with the following linear equations,

$$\Delta\beta_{x,y} = M\Delta K_1, \quad (1)$$

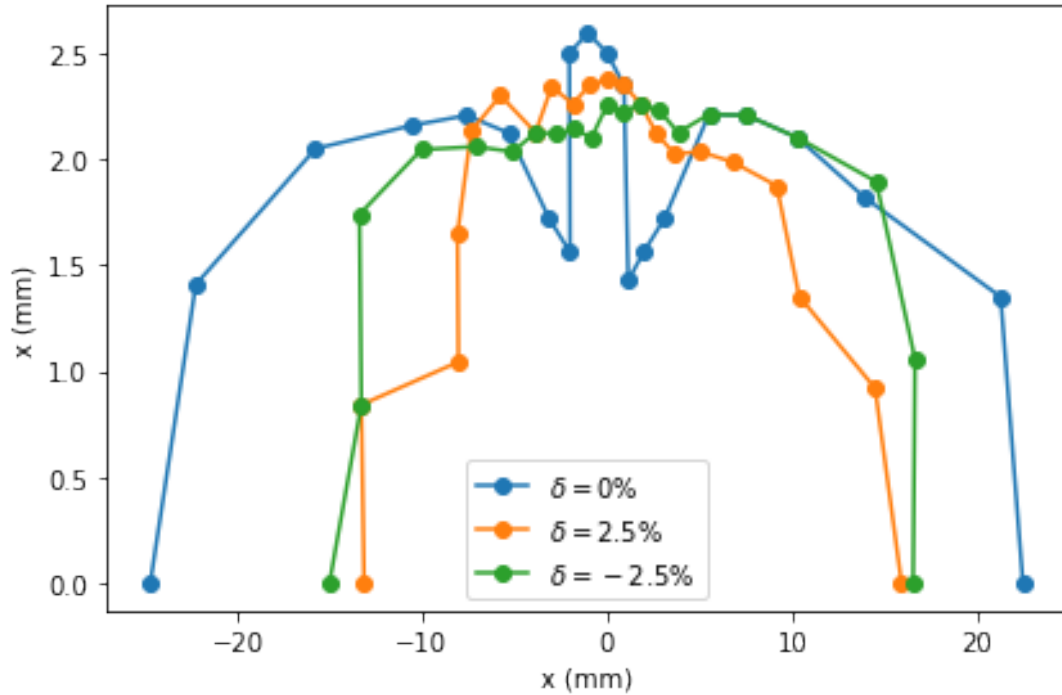


Figure 3. On- and off-momentum dynamic apertures at the injection point (with $\beta_x = 21.2\text{ m}$, $\beta_y = 3.6\text{ m}$) after integrating the HEX wiggler into the NSLS-II operation lattice. Totally 18 insertion devices are included.

here $\Delta\beta$ are the β -beat seen by 176 BPMs, $M_{(176 \times 6)}$ is the linear response matrix of β on the six knobs, ΔK_1 is the needed correction. The device was ramped up and down to calibrate the correction scheme twice, and the results were found quite reproducible as illustrated in Fig. 4.

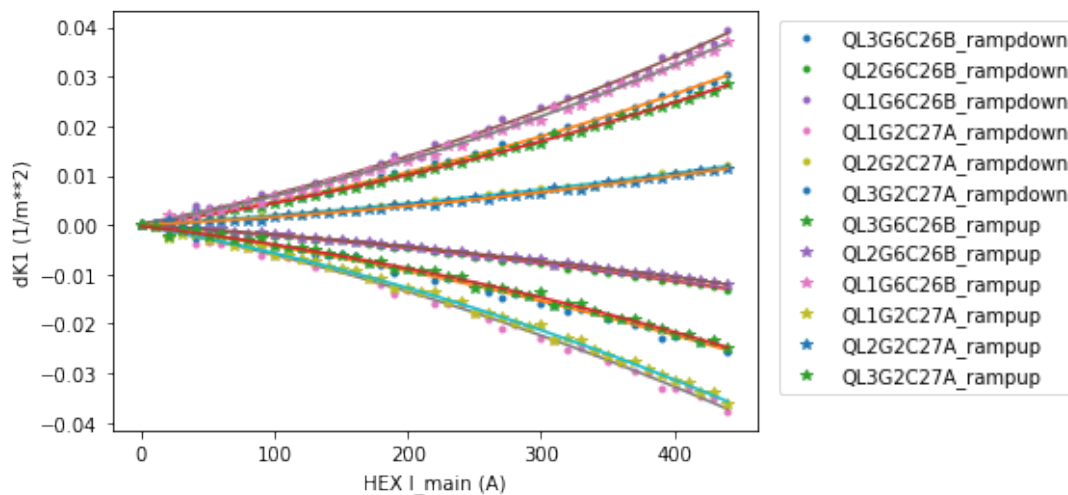


Figure 4. Calibration of the quadrupole compensation schemes for six quadrupoles when the wiggler ramps up and down. The magnet hysteresis effect is negligible.

After applying the compensation, the residual β -beats observed at those 176 BPMs (Fig. 5)

recovered to a level of 1-3%, which is similar to the status when the device was not installed. A local optics bump exists at cell 27 straight as expected, but the top-off injection efficiency was not degraded. The beam lifetime actually became longer. It is because bunches are lengthened due to an extra energy spread introduced by the wiggler, even the transverse beam emittance reduces correspondingly due to a strong radiation damping from it as well.

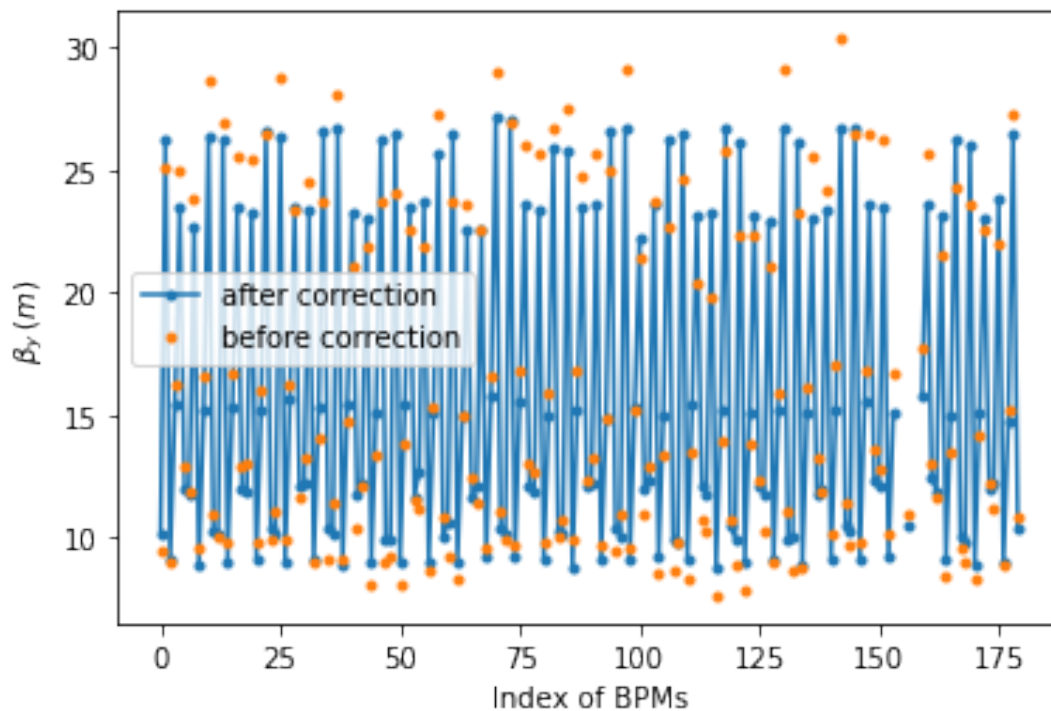


Figure 5. Vertical β -functions observed at 176 BPMs before and after implementing compensation when the main coil current is 440 A (i.e., with a peak field $B=4.34$ T). The β -functions at 4 BPMs neighboring to the wiggler are not included in the compensation scheme (as shown with blanks.)

2.3. Linear coupling characterization

The linear coupling was also measured with turn-by-turn (TBT) data when the wiggler ramped. The device was confirmed not having visible skew quadrupole components, because the linear coupling driving terms observed by BPMs are so small that it could not be resolvable. The TBT spectral analysis at 180 BPMs also show that in each transverse plane, the coupling from another plane is barely visible. As illustrated in Fig. 6, when the wiggler was excited at different currents, the Betatron tune spectrum in the transverse planes has sole peak, which confirms the coupling is too weak to be measured.

3. feedforward control of quadrupoles

To compensate the wiggler dynamically when the wiggler ramps (or a quench occurs), a feedforward control has been implemented through the EPICS control system [4]. First, an additional EPICS PV was created for each quadrupole (knob) power supply, which's setting depends on the wiggler main coil current. Six quadrupole adjustments ΔK_1 in the physics unit were converted into their power supply current, i.e., the engineering unit Ampere. Usually a

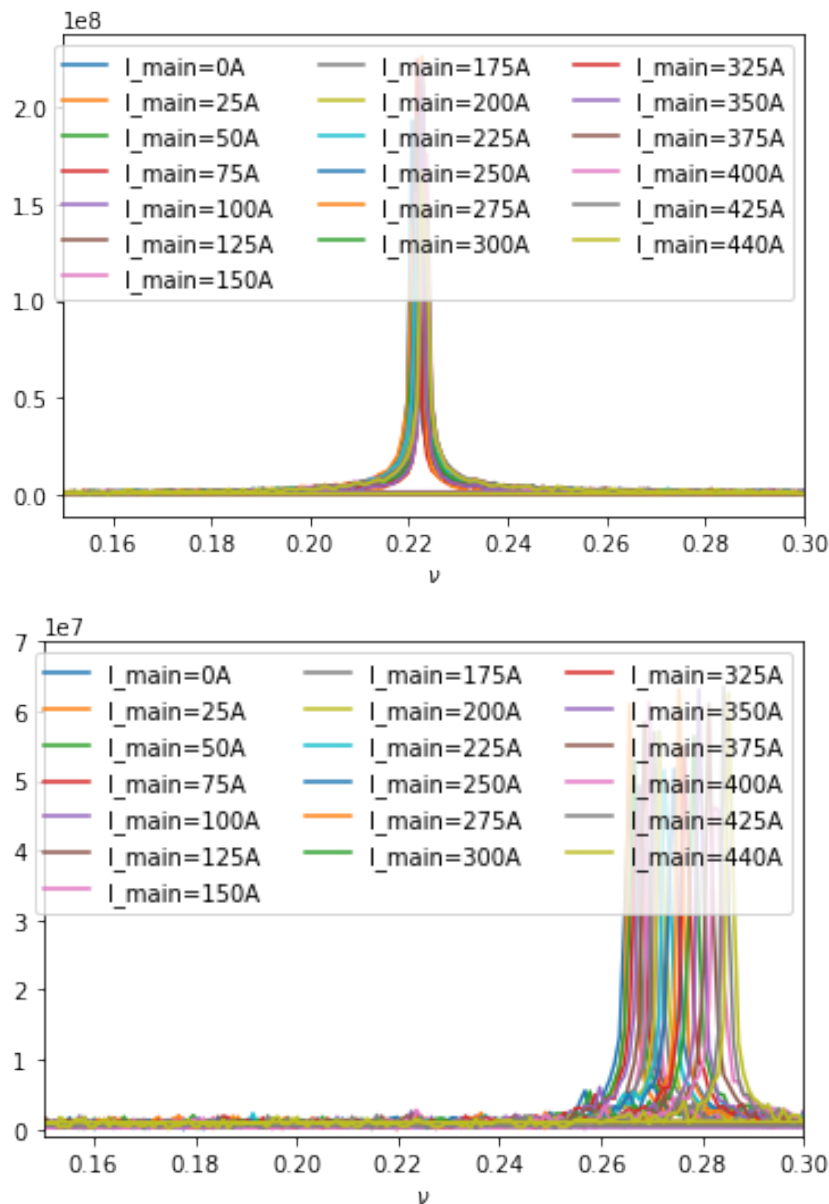


Figure 6. Spectral analysis of one of BPMs to show that the linear coupling introduced by the device is barely visible. Top: horizontal plane, bottom: vertical plane. The vertical tune shifts when the wiggler ramps because the global tune feedback is not engaged in this measurement.

ramping curve for a magnet needs to be continuous up to its second order derivatives. To smooth out the errors and discontinuity during the calibration, each quadrupole ramping curve in this control was fitted as a second order polynomial (Fig. 7).

4. CONCLUSION

A 1.2 m long superconducting wiggler with the maximum peak field 4.34 T has been installed on the NSLS-II storage ring. Its effect on the linear optics has been calibrated and compensated in the manner of a feedforward control. After the compensation, the residual *beta*-beats could be reduced down a level of 1-3%. A high efficient injection and sufficient beam lifetime indicate

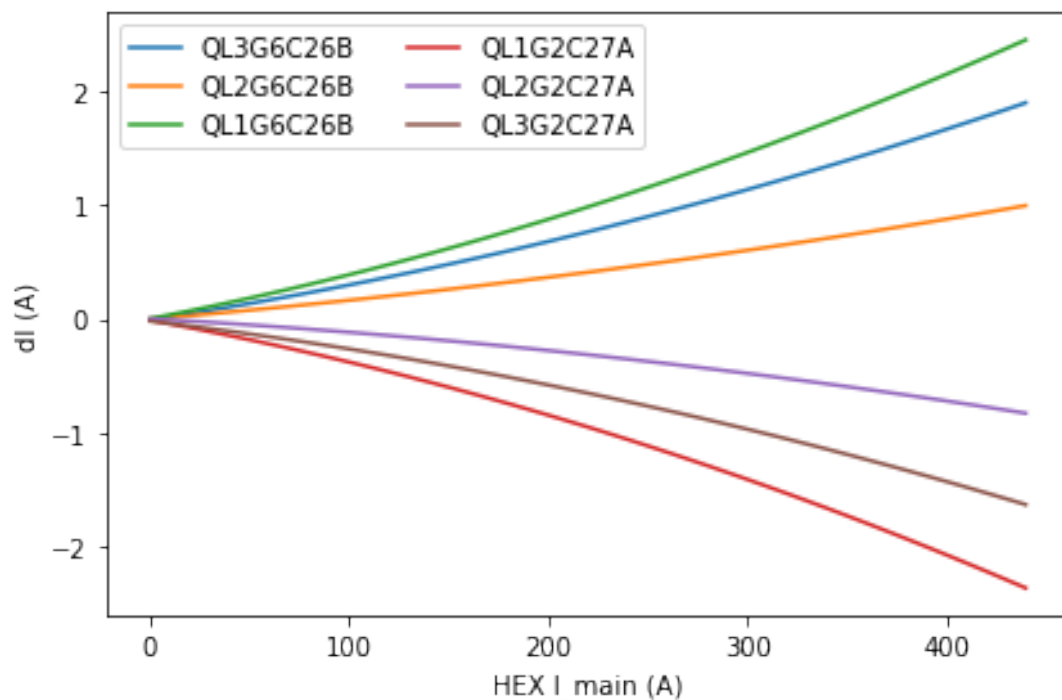


Figure 7. Linear optics feedforward control implemented with the engineering unit (A) for both the wiggler peak field and quadrupole gradients.

that the dynamic aperture and local momentum aperture were not degraded after installation.

Acknowledgments

We would like to thank our NSLS-II colleagues, who contributed to this device manufacture, installation and commissioning. This work is supported by US DOE Office of Science under Contract No. DE-SC0012704 operated by BNL.

- [1] Y. Hidaka, et al., “Commissioning of Orbit Feedforward System for HEX Superconducting Wiggler at NSLS-II,” this proceedings (2023).
- [2] P. Elleaume, “A new approach to the electron beam dynamics in undulators and wigglers,” EPAC92 661 (1992).
- [3] M. Borland, “elegant: A flexible SDDS-compliant code for accelerator simulation,” Advanced Photon Source Report, LS-287, (2000)
- [4] L.R. Dalesio, A.J. Kozubal, and M.R. Kraimer, “EPICS architecture,” Los Alamos National Lab., No. LA-UR-91-3543, (1991).